NON-LINEAR STABILITY OF CYLINDRICAL PANELS MADE OF TRANSVERSALLY FUNCTIONALLY GRADED MATERIAL WITH UNIFORMLY SHORTENED EDGES

ZBIGNIEW KOŁAKOWSKI , LESZEK CZECHOWSKI

Abstract. The present paper deals with FGM cylindrical panels with uniformly shortened edges when the shear lag phenomenon and distortional deformations are taken into account. A shell model (2D) was adopted. A method of the modal solution to the nonlinear stability problem within Koiter's asymptotic theory, using the semi-analytical method (SAM) and the transition matrix method, was applied. Post-buckling equilibrium paths for two FGM panels of step-variable gradation along the circumferential direction within the first- and second-order non-linear approximation were determined.

Key words: FGM, cylindrical panels, postbuckling equilibrium paths, first and second order approximation, step-variable graded material.

1. INTRODUCTION

In the eighties of the twentieth century, Functionally Graded Materials (FGMs) are inhomogeneous new class composites made up of two constituent phases: metallic and ceramic one. The volume fracture of both phases changes gradually along the thickness of the structures.

Birman and Byrd [1] presented a wide review of theories employed for a description of grading material properties and focus on the principal developments in functionally graded materials (FGMs) with an emphasis on the recent works published since 2000 (up to 300 works cited). Jha et al. [6] presented the review of the papers about thermoelasticity and vibration of FGM structures. The non-linear analysis of plates and shells devoted to basic types of loads is covered in [12]. The latest review paper was presented in [17].

The comparison of numerical results of the non-linear first-order theory and classical laminated plate theory applied to rectangular FGM plates is given in [16]. More results for the nonlinear post-buckling analysis of this type of elements under different types of loads are shown in [5].

Lodz University of Technology, Department of Strength of Materials, Poland

Ro. J. Techn. Sci. – Appl. Mechanics, Vol. 63, N° 3, P. 207–220, Bucharest, 2018

Static and dynamic stability of FGM plates under thermal loads were considered in, e.g. [2, 3].

In paper [13] the influence of the transverse inhomogeneity FG panels on the unsymmetrical stable post-buckling paths of cylindrical panels (i.e. the interactive effects of the two unsymmetrical post-buckling paths) is taken into account for two types of boundary conditions.

Post-buckling equilibrium paths for orthotropic materials of the strip structure in compression were defined in [11]. Thermomechnics of thin-walled FGM structures with strip arrangements was analysed in [14, 15].

In [9], on the basis of Koiter's non-linear theory of conservatory systems, it was shown that FG plate structures had non-symmetrical stable post-buckling equilibrium paths. This feature explains differences in the plate response dependence on the imperfection sign (sense). A FG plate has a non-trivial coupling matrix B. Cylindrical isotropic panels subjected to compression have unsymmetrical stable post-buckling paths.

In the present study, cylindrical panels with step-variable gradation of the material along the circumferential direction, subject to the uniform shortening of edges, are considered. Various boundary conditions on longitudinal edges were assumed. Lagrange's description, precise strains for thin-walled panels and second Piola-Kirchhoff's stress tensor, the exact transition matrix method and the numerical method of the transition matrix using Godunov's orthogonalization are used. The shear lag phenomenon and an effect of cross-sectional distortions are included. Only mechanical loads are taken account, neglecting thus the thermal ones.

2. FORMULATION OF PROBLEM

It was assumed that the materials of the panel strips were made of obeyed Hooke's law. For panels, precise geometrical relationships are assumed in order to consider both out-of-plane and in-plane bending of the panel [7, 10] (Fig. 1):

$$\begin{aligned}
\varepsilon_x &= u_{,x} + \frac{1}{2}\,(w_{,x}^2 + v_{,x}^2 + u_{,x}^2) \\
\varepsilon_y &= v_{,y} + \frac{1}{2}\,(w_{,y}^2 + u_{,y}^2 + v_{,y}^2) - w/R \\
2\varepsilon_{xy} &= \gamma_{xy} = u_{,y} + v_{,x} + w_{,x}w_{,y} + u_{,x}u_{,y} + v_{,x}v_{,y}
\end{aligned} \tag{1}$$

and

$$\kappa_x = -w_{,xx} \qquad \kappa_y = -w_{,yy} \qquad \kappa_{xy} = -2w_{,xy}. \tag{2}$$

where: u, v, w – components of the displacement vector of the panel along the x, y, z axis direction, respectively, and R – the radius of the cylindrical panel.

In the semi-analytical method (SAM), one postulates to determine approximated values of the second-order post-buckling coefficients b_{rrrr} (A3) on the basis of the linear buckling problem. The semi-analytical method (SAM) allows for the lower-bound evaluation of the second-order coefficients [8].

This approach allows the values of the first order postbuckling coefficients a_{pqr} (A3) to be precisely determined, according to the applied nonlinear Byskov and Hutchinson theory [7, 8].

The postbuckling coefficients a_{pqr} involve only buckling modes. These coefficients which are sums of integrals of different signs and they depend on the ratios of amplitude of displacements of panels. The coefficients a_{pqr} are equal to zero when the sum of the wave numbers associated with the three modes $(m_p+m_q+m_r)$ is an even number.

Table 1
Material properties of strips

Strip number	Denotation	Young's modulus E	Poisson ratio ν
		GPa	–
Strip 1	100% Al_2O_3	393	0.25
Strip 2	75% Al_2O_3+25% Al	312	0.27
Strip 3	50% Al_2O_3+50% Al	231	0.29
Strip 4	25% Al_2O_3+75% Al	151	0.31
Strip 5	100% Al	70	0.33

3. ANALYSIS OF OBTAINED RESULTS

Detailed numerical calculations were conducted for square FGM cylindrical panels under compression along the generatrix (i.e., axis x in Fig. 1). It was assumed that each panel was made of five FGM strips of the same width along the circumferential direction (axis y). The assumed material constants for each strip are listed in Table 1. Each strip is characterized by different longitudinal rigidity. Thus, the load was assumed in the form of uniform shortening of transverse edges (i.e., $u(x = 0; L = b) = \text{const.}$ – Fig. 1).

Two square panels of step-variable material transverse gradation (Fig. 1) of the following dimensions were considered:

- P1 – $L = b = 200$ mm; $t = 2$ mm;
- P2 – $L = b = 300$ mm; $t = 2$ mm;

and, moreover, for each panel, two values of the dimensionless curvature parameter $k = b^2/(Rt)$: $k = 12$ and $k = 24$ were assumed.

Two kinds of boundary conditions were assumed, namely:

- SSSS – all plate edges are freely supported:

$w(x = 0) = w(x = b) = w(y = 0) = w(y = b) = 0$;
$M_x(x = 0) = M_x(x = b) = M_y(y = 0) = M_y(y = b) = 0$;
$u(x = 0) = u(x = b) = \text{const}$; $v(x = 0) = v(x = b) = 0$;
$N_y(y = 0) = N_{xy}(y = 0) = N_y(y = b) = N_{xy}(y = b) = 0$.

- SCSC – panel transverse edges are freely supported, whereas the longitudinal ones are fixed:

$w(x = 0) = w(x = b) = w(y = 0) = w(y = b) = 0$;
$M_x(x = 0) = M_x(x = b) = 0$; $u(x = 0) = u(x = b) = \text{const}$; $v(x = 0) = v(x = b) = 0$;
$w_{,y}(y = 0) = w_{,y}(y = b) = 0$; $N_y(y = 0) = N_{xy}(y = 0) = N_y(y = b) = N_{xy}(y = b) = 0$.

Detailed numerical calculations of the panels are shown in Table 2 and Figs. 2–12.

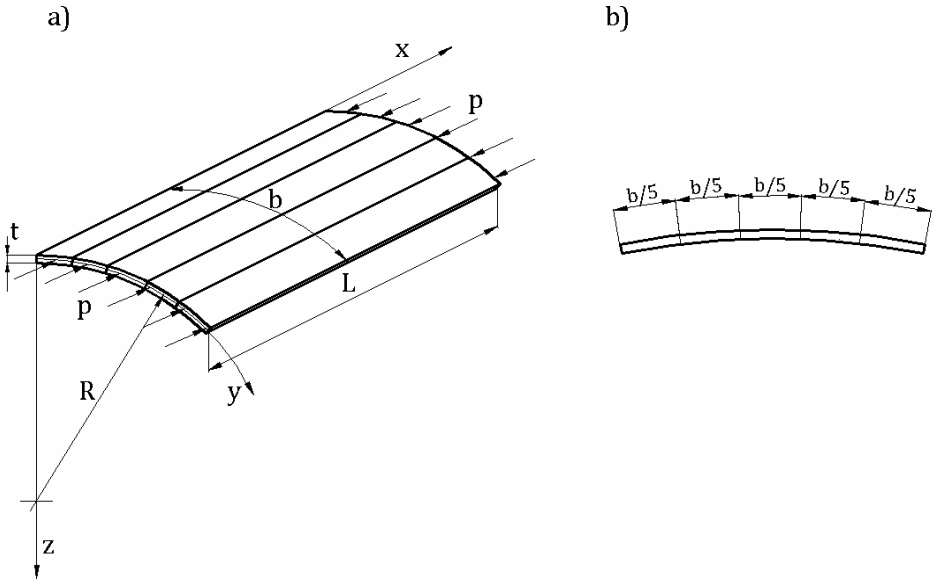

Fig. 1 – Cylindrycal panels and geometrical dimensions.

In Table 2, for the assumed dimensions and boundary conditions, values of the bifurcation loads P_r, the value r for a number of coupled modes (for uncoupled buckling $r = 1$) and the number of halfwaves m along the longitudinal direction corresponding to the given buckling mode are presented. In the case of fixed longitudinal ends, that is to say, for the case SCSC, and for the curvature parameter $k = 12$, the lowest value of the bifurcation load was attained for $m = 2$. For this case, also a bifurcation value of the load P_2 for $m = 1$ was given. For $k = 24$, lowest values of the bifurcation loads P_1 occur always for $m = 1$. As could be expected, lower values of bifurcation loads were obtained for the cases SSSS than for SCSC for the given parameter k.

Table 2
Results of critical forces

	$k = b^2/(Rt)$	Boundary conditions	r	P_r [N]	m	P_r^*/P_r	
						$\zeta_r^* = 0.01$	$\zeta_r^* = 0.1$
P-1	12	SSSS	1	43731	1	0.926	0.785
		SCSC	1	76787	2	–	–
			2	78448	1	0.941	0.827
	24	SSSS	1	79959	1	0.923	0.776
		SCSC	1	115294	1	0.932	0.802
P-2	12	SSSS	1	29179	1	0.926	0.786
		SCSC	1	51200	2	–	–
			2	52340	1	0.941	0.827
	24	SSSS	1	53466	1	0.923	0.777
		SCSC	1	77084	1	0.932	0.802

Next, the results of calculations carried out only for the first-order approximation of the applied Koiter's theory for single-mode buckling (i.e., $r = J = 1$; that is to say, in (A3) it was assumed that the nonlinear coefficients satisfied the relations: $a_{111} \neq 0$, $b_{1111} = 0$). It allows one to determine the critical loads P_r^* of real structures (i.e., with imperfections $\zeta_r^* \neq 0$) [4]. In Table 2, values of ratios of the critical loads to the respective bifurcations loads P_r^*/P_r for the assumed two values of imperfections $\zeta_r^* = 0.01$ and $\zeta_r^* = 0.1$, are given.

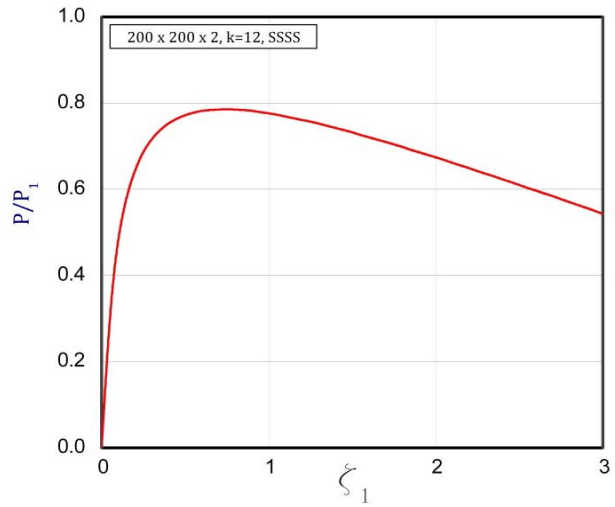

Fig. 2 – Overloading coefficient P/P_1 in function of non-dimensional deflection ζ_1 for case $b_{1111} = 0$.

This case is depicted in Fig. 2, where the dependence P/P_1 as a function of ζ_1 for SSSS and $\zeta_1^* = 0.1$ is presented. As expected, lower values of P_1^*/P_1 were attained for a higher value of imperfections. For the imperfection $\zeta_r^* = 0.1$, the values of critical loads are even by 20% lower than the values of bifurcation loads.

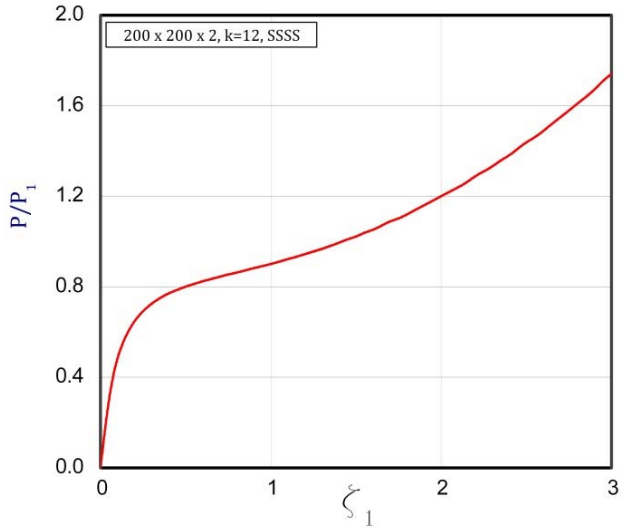

Fig. 3 – Relation P/P_1 in a function of deflection ζ_1 for case $b_{1111} \neq 0$.

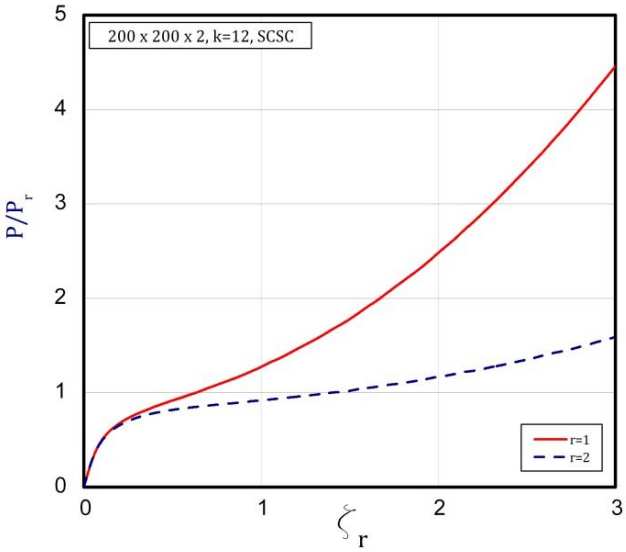

Fig. 4 – Relation of overloading P/P_1 in a function of deflection ζ_r for $r = 1$ and $r = 2$.

For the case SCSC and k = 12, the lowest bifurcation load was attained for m = 2. In this case, the post-buckling coefficient $a_{111} = 0$, thus we obtain a symmetrical post-buckling path within the first-order approximation. In the remaining cases of panels P1, we have $a_{111} \neq 0$, hence a nonsymmetrical post-buckling path was obtained [4].

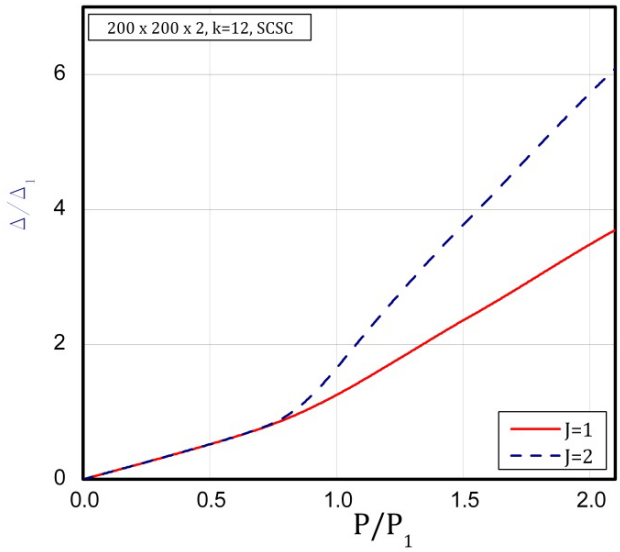

Fig. 5 – Relation of non-dimensional shortening Δ/Δ_1 in a function of overloading P/P_1.

In Fig. 3 for the case SSSS and k = 12, the post-buckling equilibrium path P/P_1 as a function of ζ_1 for the imperfection $\zeta_1^* = 0.1$ is shown. For the assumed value of imperfection, the lower and upper critical load cannot be observed.

Figure 4 presents post-buckling equilibrium paths for the uncoupled buckling for the case of SCSC and r = 1; r = 2. For r = 1 (m = 2), the post-buckling path grows faster than the path for r = 2 (m = 1). In the subsequent figure (Fig. 5), a dependence between a relative shortening of the panels Δ/Δ_1 as a function of P/P_1 is depicted for the coupled buckling (i.e., for J = 2 in (A2) and (A3)). The curve J = 1 corresponds to a single-mode buckling for (m = 2) and for $\zeta_1^* = 0.1$, whereas the curve J = 2 – to an interaction of two buckling modes, for which the following values of imperfections $\zeta_1^* = 0.1$ and $\zeta_2^* = 0.0$ were assumed. When an interaction of modes is taken into consideration, the edge shortening is higher than for the uncoupled buckling for the same value of the load P/P_1.

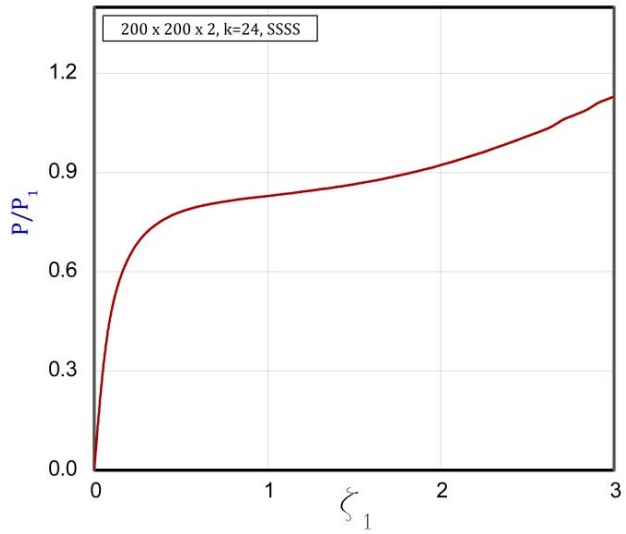

Fig. 6 – Relation P/P_1 in a function of ζ_1.

In Figs. 6 and 7, results for the curvature $k = 24$ are shown. For both kinds of the boundary conditions SSSS and SCSC, the lowest bifurcation values P_1 occur for $m = 1$. It results in the fact that both diagrams are very similar to the diagrams for $k = 12$ and $m = 1$.

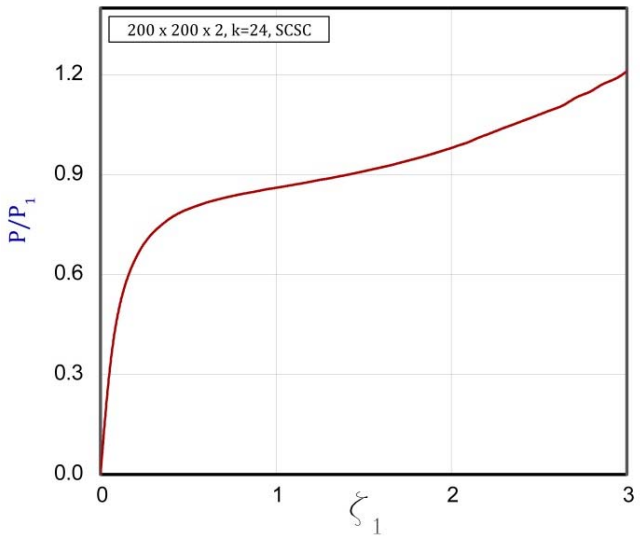

Fig. 7 – Relation P/P_1 in a function of ζ_1.

In Table 2, like for panels P1, values of the bifurcation and critical loads for two values of the curvature parameter k and two kinds of boundary conditions at the same values of imperfections as in P1 are also presented. Values of the bifurcation loads P_r for this case are lower than for the corresponding cases from P1. It is caused by the fact that the geometrical dimensions of panels P2 were increased. Values of dimensionless P_r^*/P_r are the same in practice as for P1. However, it should be remembered that the bifurcation values P_r for both the cases are different. It is evident that values of the post-buckling coefficients a_{111} and b_{1111} are close for both P1 and P2, as in equation (A3) we have the load ratios P/P_1. Plots for P1 and P2 are very similar, and thus, Fig. 8 corresponds to Fig. 3 in practice, Fig. 9 – to Fig. 4, Fig. 10 – to Fig. 5, Fig. 11 – to Fig. 6 and Fig. 12 – to Fig. 7, respectively. The curves in these figures are dimensionless, hence the dimensional quantities are different, which can be seen in Table 2 while comparing P_r for P1 and P2.

In the case when the maximal admissible compressive load is referred to the critical load of real structures (i.e., with imperfections), the maximal value of imperfection admissible by the corresponding legal regulations in force should be assumed in calculations.

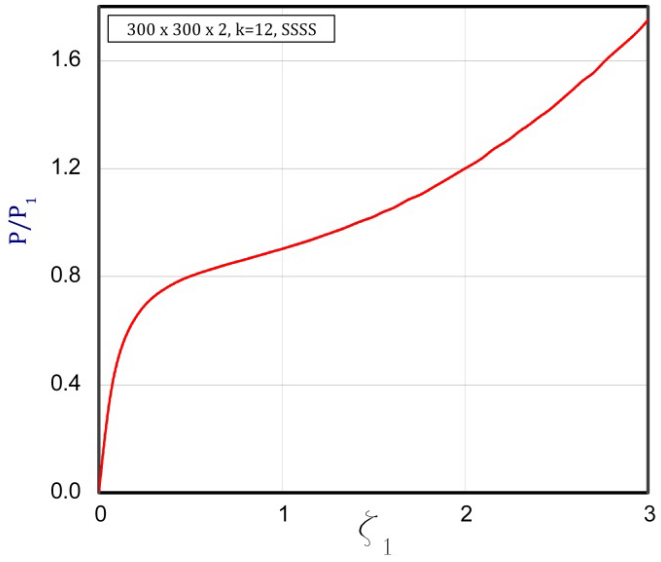

Fig. 8 – Relation P/P_1 in a function of ζ_1 for case of P_2.

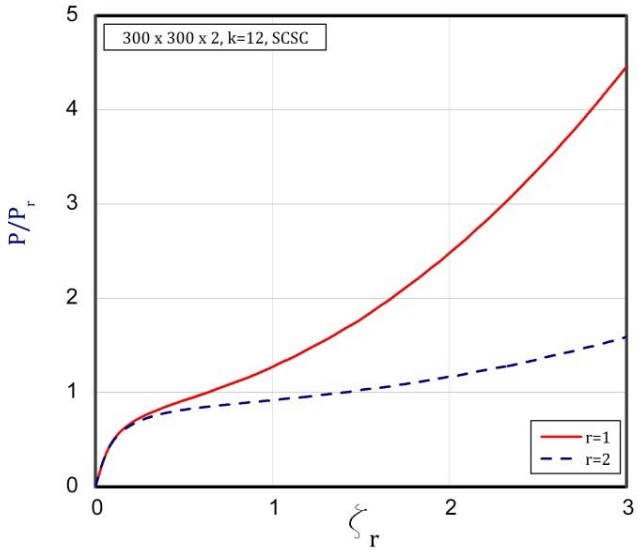

Fig. 9 – Relation of overloading P/P_r
in a function of ζ_r for $r = 1$ and $r = 2$.

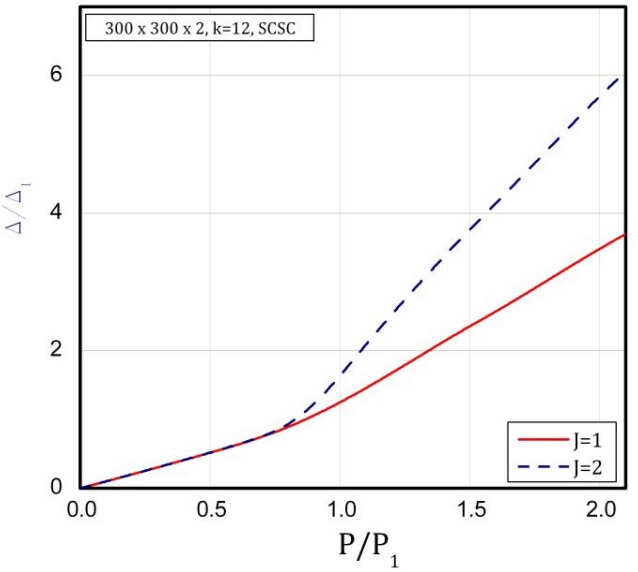

Fig. 10 – Non-dimensional shortaining D/D_1
in a function of overloading P/P_1.

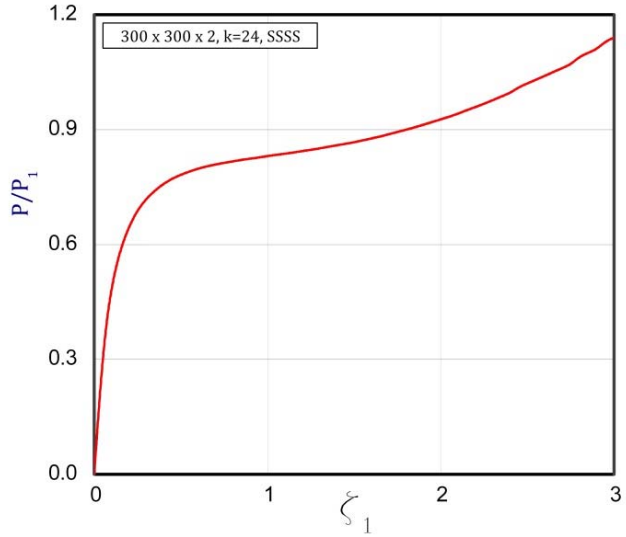

Fig. 11 – Relation P/P_1 in a function of ζ_1.

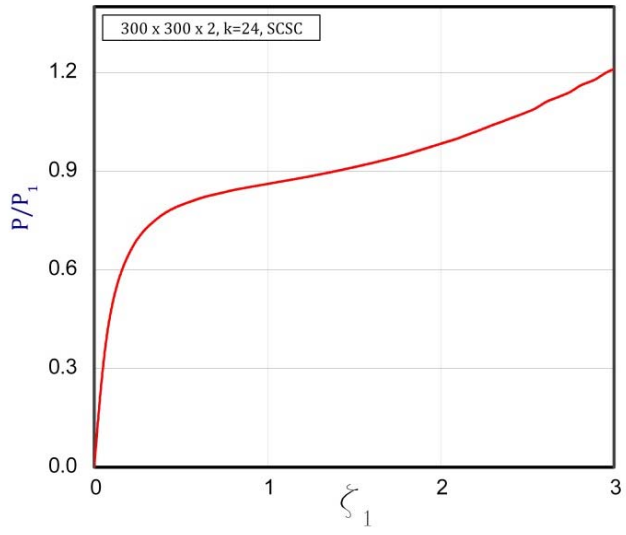

Fig. 12 – Relation P/P_1 in a function of ζ_1.

4. CONCLUSIONS

Post-buckling equilibrium paths of cylindrical FGM panels of step-variable gradation along the circumferential direction, subject to the uniform shortening of

edges along the longitudinal direction, were analysed. Two kinds of the boundary conditions on longitudinal edges were assumed: freely supported and fixed for panels of various geometrical dimensions. The problem was solved within the first- and second-order approximation. Attention was drawn to critical loads of actual panels (i.e., with imperfections) within the first-order non-linear approximation and to the fact that certain phenomena are suppressed when even numbers of buckling halfwaves occur along the longitudinal direction.

When an interaction of buckling modes is accounted for, the shortening of edges is higher than the uncoupled buckling for the same values of the overloading P/P_1. An analysis of the interactive buckling allows thus for a correct determination of the load carrying capacity of cylindrical FGM panels.

APPENDIX

The non-linear problem of an interaction between various buckling modes was solved with the asymptotic perturbation method. Let λ be a load factor. The displacement fields U and the sectional force fields N (Koiter's type expansion for the buckling problem [4, 7, 8]) were expanded into power series with respect to the dimensionless amplitude of the r-th mode deflection ζ_r (normalized in the given case by the condition of equality of the maximal deflection to the thickness of the first component plate h_1) (see [7, 8, 10]):

$$\begin{aligned} U &\equiv (u,v,w) = \lambda U_0 + \zeta_r U_r + \zeta_r^2 U_{rr} + \ldots \\ N &\equiv (N_x, N_y, N_{xy}) = \lambda N_0 + \zeta_r N_r + \zeta_r^2 N_{rr} + \ldots \end{aligned} \quad \text{for } r = 1, \ldots, J \tag{A1}$$

where the pre-buckling (i.e., unbending) fields are U_0, N_0, the first non-linear order fields are U_r, N_r (eigenvalues problems) and the second non-linear order fields – U_{rr}, N_{rr}, respectively. The range of indices is [1, J], where J is a number of interacting modes.

For thin-walled structures with the geometric imperfections $\overline{U}$ (only the linear initial imperfections determined by the shape of the r-th buckling modes), the total potential energy h can be written in the form [7, 8]:

$$\begin{aligned} \Pi = &-\frac{1}{2}\left(\frac{P}{P_r}\right)^2 \overline{a}_0 + \frac{1}{2}\sum_{r=1}^{J} \overline{a}_r \zeta_r^2 \left(1 - \frac{P}{P_r}\right) + \frac{1}{3}\sum_{p}^{J}\sum_{q}^{J}\sum_{r}^{J} \overline{a}_{pqr}\zeta_p\zeta_q\zeta_r + \\ &+ \frac{1}{4}\sum_{r}^{J} \overline{b}_{rrrr}\zeta_r^3 - \sum_{r}^{J} \frac{P}{P_r}\overline{a}_r\zeta_r^*\zeta_r \end{aligned} \tag{A2}$$

and the equilibrium equations corresponding to (A2) are as follows:

$$\left(1-\frac{P}{P_r}\right)\xi_r + a_{pqr}\xi_p\xi_q + b_{rrrr}\xi_r^3 = \frac{P}{P_r}\xi_r^* \text{ for } r = 1, \ldots, J \tag{A3}$$

where: P is the applied force, P_r, ζ_r, ζ_r^* – the buckling force of the r-th buckling mode, the dimensionless amplitude of the r-th buckling mode and the dimensionless amplitude of the initial deflection corresponding to the r-th buckling mode, respectively. The coefficients $\overline{a}_0$, $\overline{a}_r$, $\overline{a}_{pqr}$ and $\overline{b}_{rrrr}$ can be determined with the equations described in the literature [7-10].

The following notations are introduced in (A3):

$$a_{pqr} = \overline{a}_{pqr} / \overline{a}_r,\ b_{rrrr} = \overline{b}_{rrrr} / \overline{a}_r. \tag{A4}$$

A relative shortening Δ/Δ_1 of the panel on the support as a function of the P/P_1 load has the following form:

$$\frac{\Delta}{\Delta_1} = \frac{P}{P_1}\left[1 + \frac{P_1}{P\overline{a}_0}\sum_{r=1}^{J}\frac{P_1}{P_r}\overline{a}_r\zeta_r\left(0.5\zeta_r + \zeta_r^*\right)\right] \tag{A4}$$

where Δ_1 – the buckling shortening of the panel, corresponding to the minimal value of the buckling force P_1.

Acknowledgements. The work was carried out thanks to the financial support of the National Science Centre of Poland (UMO-2017/25/B/ST8/01046).

Received on October 15, 2018

REFERENCES

1. BIRMAN, V., BYRD, L.W., *Modeling and analysis of functionally graded materials and structures*, Appl. Mech. Rev., **60**, *5*, pp. 195–216, 2007.
2. CZECHOWSKI, L., KOWAL-MICHALSKA, K., *Static and dynamic buckling of rectangular functionally graded plates subjected to thermal loading. Strength of Materials*, **45**, *6*, pp. 666–673, 2013.
3. CZECHOWSKI, L., *Analysis of dynamic response of functionally graded plate due to temperature pulse load*, Composite Structures, **160**, pp. 625–634, 2017.
4. VAN DER HEIJDEN, A.M.A., *W.T. Koiter's Elastic Stability of Solids and Structures*, Cambridge University Press, 2008.
5. HUI-SHEN, S., *Functionally graded materials – Nonlinear analysis of plates and shells*, CRC Press, Taylor & Francis, London, 2009.
6. JHA, D.K., KANT, T., SINGHT, R.K., *A critical review of recent research on functionally graded plates*, Composite Structures, **96**, pp. 833–849, 2013.

7. KOŁAKOWSKI, Z., KRÓLAK, M., *Modal coupled instabilities of thin-walled composite plate and shell structures*, Composite Structures, **76**, pp. 303–313, 2006.
8. KOŁAKOWSKI, Z., MANIA, R., *Semi-analytical method versus the FEM for analysis of the local post-buckling of thin-walled composite structures*, Composite Structures, **97**, pp. 99–106, 2013.
9. KOŁAKOWSKI, Z., MANIA, R., GRUDZIECKI, J., *Local nonsymmetrical postbuckling equilibrium path of the thin FGM plate*, Eksploatacja i Niezawodnosc – Maintenance and Reliability, **17**, *1*, pp. 135–142, 2015.
10. KOŁAKOWSKI, Z., TETER, A. *Load carrying capacity of functionally graded columns with open cross-sections under static compression*, Composite Structures, **129**, pp. 1–7, 2015.
11. KUBIAK, T., *Postbuckling behavior of thin-walled girders with orthotropy varying widthwise*, Int. J. Solids Structures, **38**, pp. 4839–4855, 2001.
12. LIEW, K.M., ZHAO X., FERREIRA, A.J.M., *A review of meshless methods for laminated and functionally graded plates and shells*, Composite Structures, **93**, *8*, pp. 2031–2041, 2011.
13. LYKHACHOVA, O., KOŁAKOWSKI, Z., *Influence of the transverse inhomogeneity on the nonlinear post-buckling path of compressed FG cylindrical panels*, Engineering Transactions, **65**, *4*, pp. 563–578, 2017.
14. OSTROWSKI, P., MICHALAK, B., *The combined asymptotic-tolerance model of heat conduction in a skeletan micro-heterogeneous hollow cylinder*, Composite Structures, **134**, pp. 343–352, 2015.
15. OSTROWSKI, P., MICHALAK, B., *A contribution to the modelling of heat conduction for cylindrical composite conductors with non-uniform distribution of constituents*, Int. J. Heat and Mass Transfer, **92**, pp. 435–448, 2016.
16. REDDY, J.N., *Analysis of functionally graded plates*, Int. J Numer. Meth. Eng., **47**, pp. 663–684, 2000.
17. SWAMINATHAN, K., NAVEENKUMAR, D.T., ZENKOUR, A.M., CARRERA, E., *Stress, vibration and buckling analyses of FGM plates – A state-of-the-art review*, Composite Structures, **120**, pp. 10–31, 2015.